

**DETERMINATION OF MODE I FRACTURE BEHAVIOR OF SOUTHERN
YELLOW PINE (*PINUS TAEDA* L.) WOOD USING SINGLE-EDGE-NOTCHED
BENDING TEST**

ARIF CAGLAR KONUKCU
IZMIR KATIP CELEBI UNIVERSITY
TURKEY

(RECEIVED AUGUST 2021)

ABSTRACT

The fracture behavior of southern yellow pine (*Pinus taeda* L.) was experimentally analyzed in the radial-longitudinal and the radial-tangential crack propagation systems using a single-edge-notched bending test method in mode I loading condition. Three fracture parameters, the initial slope, the fracture toughness, and the specific fracture energy, were determined from the obtained load-deformation curves of each test sample. The results were statistically analyzed and compared with each other using the independent samples t-test. The radial-longitudinal crack propagation system had a significantly greater fracture toughness than in the radial-tangential crack propagation system. The stiffness in the radial-longitudinal system was also significantly higher than in the radial-tangential system. It was observed that the crack growing in the tangential direction needed more energy per unit area to separate a wood sample into two halves. However, there was no significant difference between the specific fracture energy values of crack propagation systems.

KEYWORDS: Fracture toughness, southern yellow pine, specific fracture energy.

INTRODUCTION

The fracture toughness is a geometry-independent material property of wood (Mall et al. 1983, Tan et al. 1995). Orthotropic materials like wood have unique and independent mechanical properties in three different grain orientations of longitudinal (L), radial (R), and tangential (T). Therefore, wood has different fracture behaviors in its different grain orientations. Orthotropic materials have typical six crack propagation systems as shown in Fig. 1. Each of the six systems is defined by two letters; i.e., the first letter indicates the grain orientation perpendicular to the crack plane, whereas the second letter indicates the direction of crack propagation, for instance, RT indicates the system has its crack growing in the tangential direction on the radial direction

perpendicular to the crack plane. Three basic fracture modes can be used for performing the fracture toughness test based on three different loading conditions as shown in Fig. 2: mode I (tensile mode), mode II (in-plane shear mode), and mode III (out-of-plane shear mode). The mode I is typically the dominant case and the most dangerous condition for most materials (Smith et al. 2003). The mode I and mode II are commonly seen in wooden structures (Patton-Mallory and Cramer 1987).

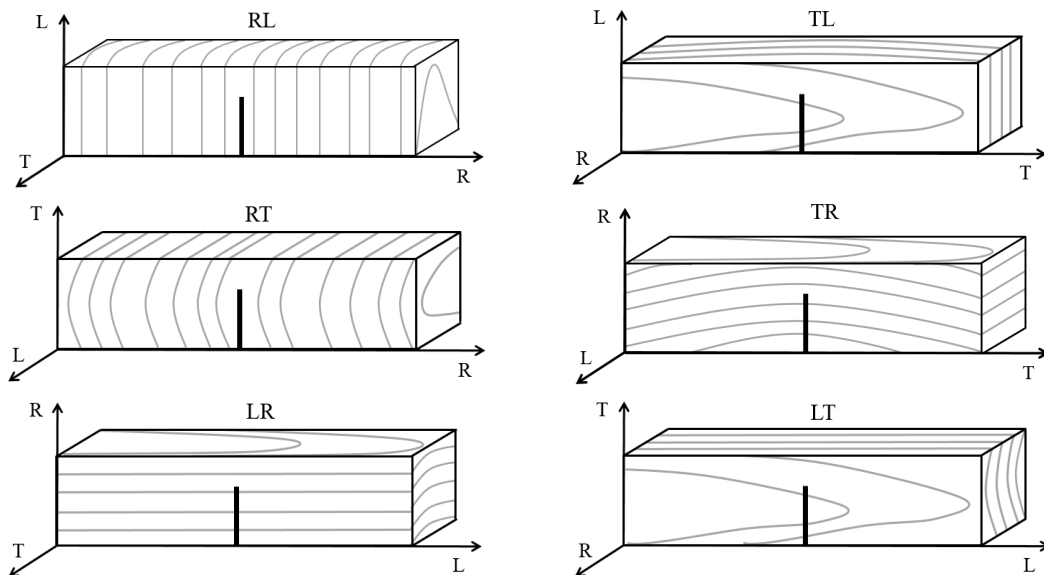
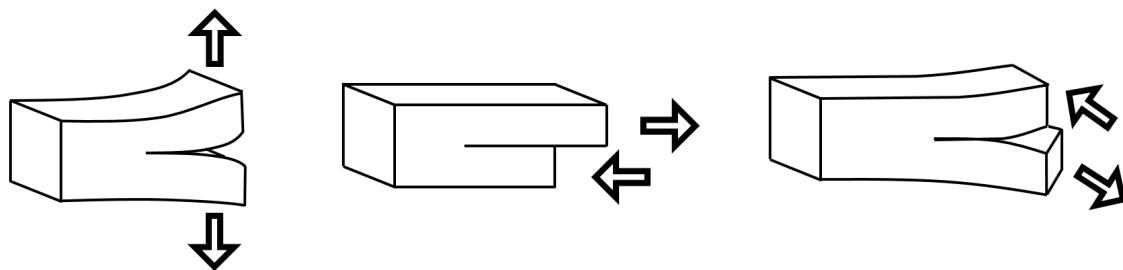


Fig. 1: Typical six crack propagation systems for wood. L: longitudinal, R: radial, and T: tangential.



(a) Mode I – tension.

(b) Mode II – in-plane shear.

(c) Mode III – out-of-plane shear.

Fig. 2: The illustration of the three basic fracture modes subjected to a tensile load (a), an in-plane shear load (b), and an out-of-plane shear load (c).

The ASTM E399-90: 2009 standard for metallic materials is taken as the reference in previous studies since there has been no standard test method for measuring fracture toughness of wood. The standard proposes three configured tests of loading specimens for measuring fracture toughness in mode I, i.e., single-edge-notched bending (SENB) (Nakao et al. 2012, Watanabe et al. 2011, Yoshihara 2010a), single-edge-notched tension (SENT) (Yoshihara 2010b), and compact tension (CT) (Fonselius and Riipola 1992, Kretschmann 2008, Ohuchi et al. 2011, Thuvander and Berglund 2000). SENB test is a single-edge-notched and fatigue

pre-cracked beam loaded in three-point bending, commonly used for measuring fracture toughness of wood in mode I (Schniewind and Centeno 1973, Smith et al. 2003).

The fracture behavior of wood is strongly influenced by its grain orientation (Kretschmann et al. 1991, Qiu et al. 2012, Smith et al. 2003) although it is affected by its microstructure, its density, and environmental conditions such as relative humidity (RH) and temperature (Ashby et al. 1985, Boatright and Garrett 1983, Johnson 1973, Mall et al. 1983, Patton-Mallory and Cramer 1987, Porter 1964). Many studies reporting the effect of grain orientations of wood on fracture toughness have been appeared in the literature (Barrett 1976, Ohuchi et al. 2011, Schniewind and Centeno 1973). Schniewind and Centeno (1973) studied the fracture toughness of air-dry Douglas fir wood in all six crack propagation systems and determined that the fracture toughness in LT and LR crack propagation systems were significantly higher (ranged from 2.42 to 2.69 MPa.m^{1/2}) than the other four systems (in RL, RT, TL, and TR systems ranged from 0.31 to 0.41 MPa.m^{1/2}). The four crack propagation systems in wood are received the most attention because each of these four crack propagation systems has lower strength and stiffness in the radial and tangential directions perpendicular to the crack plane (Kretschmann 2010). Moreover, Qiu et al. (2012) mentioned that the RL and RT crack propagation systems were the common cracks observed in wood composites because their low strength in tension perpendicular to grain.

The initial slope indicates the stiffness of the species, whereas the specific fracture energy characterizes the whole fracture process until the complete separation of surfaces (Smith et al. 2003). The TL, RL, RT, and TR crack propagation systems have lower fracture parameters because the wood has weak planes in parallel to the grain (Boatright and Garrett 1983). Reiterer et al. (2002) investigated that fracture characteristics of four wood species, one softwood (spruce) and three hardwoods (alder, oak, and ash), in RL and TL crack systems under loading perpendicular to the grain. It was found that softwood had completely more stable crack propagation than hardwoods because hardwoods had shorter fibers than softwoods and had multiseriate rays caused by energy-dissipating processes like fiber bridging. They also concluded that the stiffness and the resistance against crack initiation in the RL system were higher than in the TL system. Tukiainen and Hughes (2016) also studied the fracture behavior of spruce and birch wood in RT and TR crack systems subjected to pure mode I loading. Based on the results, the stiffness, the resistance against crack initiation, and the fracture energy required to grow the crack were higher in the RT system than in the TR system due to the effect of the rays. In general, the structure of softwoods is more uniform with containing 90-95% long tracheids and about 5-7% rays of the total volume (Shmulsky and Jones 2011). Rays in southern yellow pine are only one cell wide and about 195 µm high, whereas rays in most hardwood species are one to five cells wide and < 1 mm high (Wiedenhoeft 2010). Therefore, softwood rays are of little significance to mechanical properties although they are important to tree functions (Smith et al. 2003).

Although the fracture toughness is a material property, the fracture behavior can be seen different for different modes (mode I, mode II, and mode III) and different crack propagation systems of wood (LR, LT, RL, RT, TR, and TL). Therefore, this study investigated the fracture behavior of southern yellow pine wood under pure mode I loading in the RL and RT crack propagation systems using the SENB test method. In particular, the initial slope, the fracture

toughness, and the specific fracture energy were determined from the obtained load-deformation curves. Moreover, differences between the two crack propagation systems were analyzed and discussed.

MATERIAL AND METHODS

Material

Southern yellow pine (*Pinus taeda* L.) (SYP) quarter sawn lumber was investigated in this study. The lumber was selected on the basis of straight-grain and free from defects. The single-edge-notched bending (SENB) test specimens as shown in Fig. 3 were prepared with the initial crack length in the parallel to the grain in the RL as well as in the RT system. The size of SENB test specimen was defined as $W = 20$ mm, $a = 10$ mm, and $B = 15$ mm. A one mm thick crack was first cut using band saw to create the initial crack and then it was extended a 1 mm long sharp crack tip using a razor blade. Fifteen samples were prepared for each crack propagation system. All testing samples were placed in the conditioned humidity chamber with its condition controlled at a temperature of 20°C and relative humidity of 42% until an equilibrium moisture content of approximately 8% was reached prior to fracture toughness testing. The average measured density of the wood at 8% moisture content (MC) was 480 ± 37 kg m⁻³.

Methods

There is no standard test method for determining the fracture toughness of wood. Therefore, the ASTM E399-09: 2009 of metallic materials was taken as the reference of the test. Fig. 3 shows the general configuration of test setup for a SENB test on a fracture toughness testing block in reference to ASTM E399-09: 2009. The test was performed on an INSTRON 5566 universal test machine. The load P was applied at mid-span with a crosshead speed of 1 mm min⁻¹ (Yoshihara 2010a). Load-deformation (P - δ) curves of all tested specimens loaded until the complete separation of surfaces occurred were recorded. Three fracture parameters were obtained from the P - δ curves i.e., the fracture toughness (K_{IC}), the initial slope (k_{init}), and the specific fracture energy (G_f). The fracture toughness, K_{IC} (MPa.m^{1/2}), was calculated using the following formula:

$$K_{IC} = \frac{P_Q + S}{B \cdot W^{3/2}} * f\left(\frac{a}{W}\right) \quad (1)$$

where:

$$f\left(\frac{a}{W}\right) = 3 * \sqrt{\frac{a}{W}} * \frac{1.99 - \left(\frac{a}{W}\right) * \left(1 - \frac{a}{W}\right) \left[2.16 - 3.92 * \frac{a}{W} + 2.7 * \left(\frac{a}{W}\right)^2\right]}{2 * \left(1 + 2 * \frac{a}{W}\right) * \left(1 - \frac{a}{W}\right)^{3/2}} \quad (2)$$

where: P_Q is the failure load initiating crack propagation (N), S is the span length, B is the thickness of a SENB test specimen (m), W is the width of a SENB test specimen (m), a is the initial crack length (m) (Fig. 3).

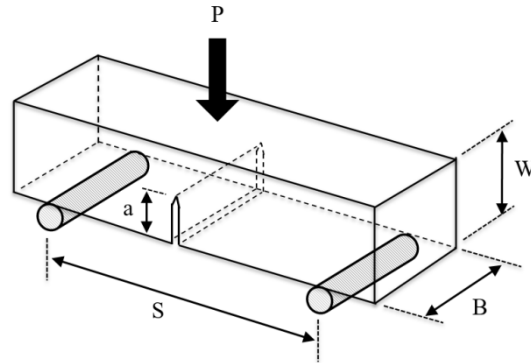


Fig. 3: The general configuration of test setup for SENB test.

The failure load initiating crack propagation, P_Q , in Eq. 1 was determined using the following steps: (1) drawing a tangential line to the initial linear portion of the curve, (2) offsetting this line by a 5% reduction in its slope, and (3) locating the intersection of this offsetting line with the curve (ASTM E399-09: 2009). The failure load was defined if the maximum load was found earlier than the intersection (Fig. 4b).

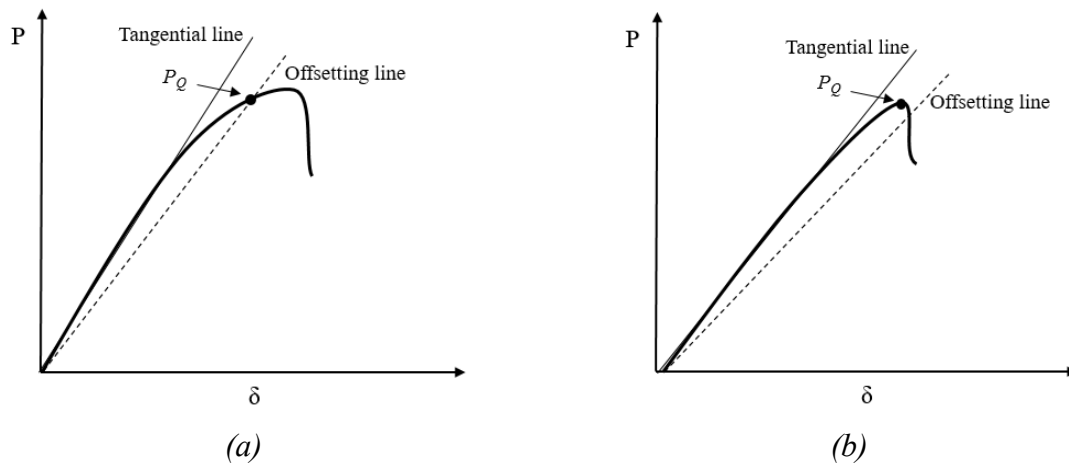


Fig. 4: Graphical illustration of how to determine the failure load initiating crack propagation, P_Q , based on the load-deformation curve of a tested specimen: the intersection before (a), and after (b) the maximum load.

To characterize the stiffness of the wood, the initial slope, k_{init} ($\text{N}\cdot\text{m}^{-1}$), of the P - δ curves in the linear elastic region was determined using the following formula (Majano et al. 2010, Reiterer et al. 2002, Reiterer and Tschegg 2002):

$$k_{init} = \frac{\Delta P}{\Delta \delta} \quad (3)$$

where: ΔP is the difference between the upper and lower limit of load within the linear elastic region (N), $\Delta \delta$ is the deflection difference corresponding to ΔP (mm) (Fig. 5).

The specific fracture energy G_f (Jm^{-2}) that represents the work required to separate the fracture surfaces, was calculated from the integrated area under the whole P- δ curve (Fig. 5) divided by the area of the fracture surface using the following formula (Majano et al. 2010, Reiterer et al. 2002, Reiterer and Tschegg 2002):

$$G_f = \frac{1}{(W-a) \cdot B} \int_0^{\delta_{max}} P(\delta) d\delta \quad (4)$$

where: P is the applied load (N), δ is the deflection at the loading point, W is the width of the test specimen (m), a is the initial crack length (m), B is the thickness of the test specimen (m).

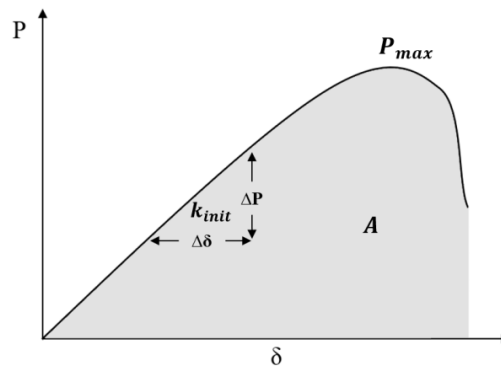


Fig. 5: Graphical illustration of how to define the initial slope, k_{init} , and the integrated area A , based on the load-deformation curve.

Independent samples t-test at 95% level of confidence was performed to determine whether there were significant differences between the crack propagation systems, the RL and the RT, tested in this study. All statistical analyses were carried out using the SAS 9.4 statistical software.

RESULTS AND DISCUSSION

Typical load-deformation curves obtained by the SENB tests of SYP in the RL and RT crack propagation systems are shown in Fig. 6. The curves can clearly illustrate the effect of crack propagation systems on fracture behaviors.

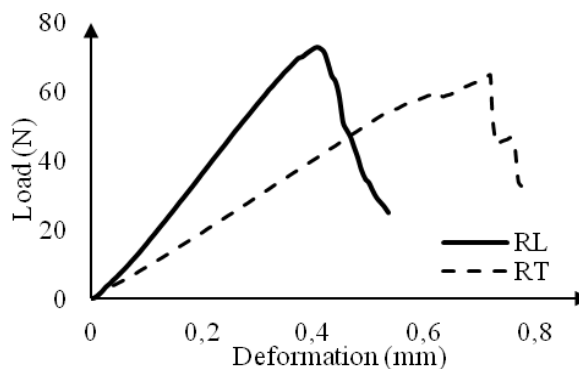


Fig. 6: Typical load-deformation curves obtained by the SENB test in the RL and RT crack propagation systems.

Based on the curves, SYP showed stable crack propagation until the complete separation of the specimens for the RL and RT systems. The maximum loads in the load-deformation curve for all specimens in both crack systems were defined as the failure loads because the load was found earlier than the intersection drawn with a 5% reduction in initial slope (Fig. 4b). In general, the failure load in the RL crack system has higher than in the RT crack system.

The effect of crack propagation systems on fracture behavior was quantified with the fracture toughness K_{IC} , the initial slope k_{init} , and the specific fracture energy Gf , and the results are summarized in Tab. 1. In order to characterize the fracture toughness of wood in both crack systems according to Eq. 1 was determined from the failure load. Mean comparison results indicated that in general, the RL crack system had higher fracture toughness value of $0.36 \text{ MPa}\cdot\text{m}^{1/2}$ (or failure load value of 71.93 N) than the RT crack system. The fracture toughness value in the RT crack propagation system was significantly lower than that in the RL system ($p < 0.05$), indicating that cracks perpendicular to the radial direction initiate tangentially easier than they do longitudinally. The initial slope is characteristic for the elastic properties and proportional to an effective modulus of elasticity (Harmuth et al. 1996, Reiterer et al. 2002). The initial slope of the RL specimen was higher than that of the RT specimen. The results obtained from the independent samples t-test also indicated a significant difference between the means of the initial slope of both crack systems ($p < 0.05$). This finding indicates that the modulus of elasticity would be expected higher under mode I loading in the RL crack propagation system than in the RT.

Tab. 1: Mean comparisons of fracture parameters in the RL and RT crack propagation systems.

Fracture parameter	Crack propagation system	Mean	SD	SE	COV	t_{value}	Sig. (2-tailed)
Failure load (N)	RL	71.93	10.06	2.5971	0.14	2.13	0.0420
	RT	65.58	5.65	1.4600	0.09		
Fracture toughness ($\text{MPa}\cdot\text{m}^{1/2}$)	RL	0.36	0.05	0.0130	0.14	2.32	0.0282
	RT	0.33	0.03	0.0078	0.09		
Initial slope ($\text{N}\cdot\text{m}^{-1}$)	RL	156.67	38.32	9.8947	0.24	6.18	< 0.0001
	RT	92.04	13.08	3.3761	0.14		
Specific fracture energy ($\text{J}\cdot\text{m}^{-2}$)	RL	209.97	46.53	12.013	0.22	-1.54	0.1348
	RT	231.51	27.73	7.1603	0.12		
Brittleness (mm)	RL	16.44	2.24	0.5793	0.14	-4.36	0.0002
	RT	20.56	2.89	0.7463	0.14		

SD - standard deviation, SE - standard error, COV - coefficient of variation.

The specific fracture energy is separated into crack initiation and crack propagation energies (Smith et al. 2003). Crack initiation energy is the energy required to develop a fracture process zone and causes to create micro-cracks and irreversible deformations around the crack tip. On the other hand, crack propagation energy is the energy that is dissipated through the formation of microcracks that ultimately turn into the main crack (Majano et al. 2010, Reiterer and Tschegg 2002, Smith et al. 2003). Mean comparison for the specific fracture energy was listed in Tab. 1. The RT crack system had a higher specific fracture energy value of $231.51 \text{ J}\cdot\text{m}^{-2}$ than the RL crack system ($209.97 \text{ J}\cdot\text{m}^{-2}$). It means that the crack growing in the tangential direction needed

more energy per unit area to separate a wood sample into two halves. However, there was no significant difference between the means of crack propagation systems with a $p = 0.1348$. Fig. 7 shows average data points and boxplots to illustrate trends. Boxplots show the minimum, the 25th percentile, the median, the 75th percentile, and the maximum points.

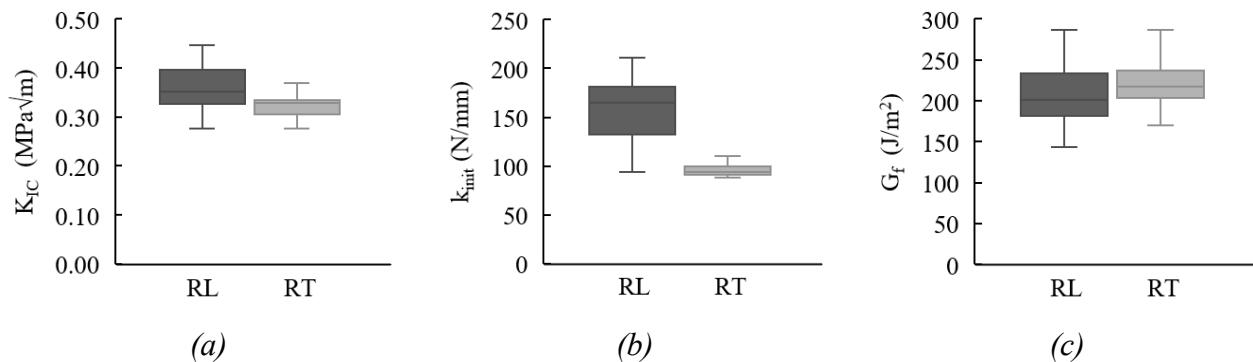


Fig. 7: Boxplots of the fracture toughness (a), the initial slope (b), and the specific fracture energy (c) of SYP obtained by the SENB in the RL and RT crack propagation systems.

Majano et al. (2010) pointed out that increasing the specific fracture energy leads to an increase in ductility. Reiterer and Tschegg (2002) also indicated that the ductility increased with increasing both the dissipated energy during the crack initiation and the crack propagation. The failure load, the initial slope, and the specific fracture energy were combined to obtain a brittleness number to characterize whether the material behavior is more ductile or brittle (Reiterer et al. 2002, Tschegg et al. 2001). Lower brittleness number indicates that the material behavior is more ductile. The results show that the RL crack system acted more ductile behavior than the RT crack system although the RT crack system had higher specific fracture energy than the RL crack system. The reason could be explained by 80% of the RT test blocks in this study had the initial crack within the latewood region whereas the initial crack within the earlywood region was dominant for the RL crack system. The specific fracture energy is not independent of the loading mode or crack propagation system for one species; therefore, it may be influenced by other parameters such as the density (Fruhmann et al. 2002). Konukcu et al. (2021) mentioned that the mode I fracture behavior of the wood can be affected by not only its density but also could be its microstructure. Previous studies mentioned that significant differences in mechanical properties exist between earlywood and latewood (Kang et al. 2014, Kretschmann and Cramer 2007) because the cells of latewood have thick walls with small cell cavities while the cells of earlywood have thin walls with large cell cavities (Kang et al. 2014, Thuvander and Berglund 2000). Ohuchi et al. (2011) also found higher fracture parameters for the TR crack system than for the RT crack system because the crack of the TR was progressing through the latewood region whereas the crack of the RT was growing within the earlywood region.

CONCLUSION

In this study, the fracture behavior of SYP was experimentally analyzed in the RL and the RT crack propagation systems using the SENB test method in mode I. The failure load was used to calculate the fracture toughness whereas the load-deformation curves were used to determine the initial slope and the specific fracture energy. The following conclusions from the results of the study can be made. The Independent samples t-test showed that the fracture toughness indicating the resistance against crack initiation and the initial slope indicating the stiffness were significantly higher in the RL than in the RT. The specific fracture energy of the RL was lower than that of the RT, but this difference was not significant. It means that more energy per unit area for the RT was needed to separate a wood sample into two halves. It was also found that the behavior of SYP in the RL crack system became more brittle than in the RT. Differences in the fracture behavior of SYP depending on the crack propagation systems could be explained by structural features of the tested samples, especially the crack tip position in a growth ring of wood.

ACKNOWLEDGMENTS

The author would like to thank to the Department of Sustainable Bioproducts at Mississippi State University for providing experimental facilities.

REFERENCES

1. Ashby, M.F., Easterling, K.E., Harrysson, R., Maiti, S.K., 1985: The fracture and toughness of woods. *Proceedings of the Royal Society of London A: Mathematical, Physical and Engineering Sciences* 398(1815): 261–280.
2. ASTM E399-09, 2009: Standard test methods for linear-elastic plane-strain fracture toughness K_{Ic} of metallic materials.
3. Barrett, J.D., 1976: Effect of crack-front width on fracture toughness of Douglas-fir. *Engineering Fracture Mechanics* 8(4): 711–717.
4. Boatright, S.W.J., Garrett, G.G., 1983: The effect of microstructure and stress state on the fracture-behavior of wood. *Journal of Materials Science* 18(7): 2181–2199.
5. Fonselius, M., Riipola, K., 1992: Determination of fracture toughness for wood. *Journal of Structural Engineering* 118(7): 1727–1740.
6. Fruhmann, K., Reiterer, A., Tschegg, E.K., Stanzl-Tschegg, S.S., 2002: Fracture characteristics of wood under mode I, mode II, and mode III loading. *Philosophical Magazine A* 82(17–18): 3289–3298.
7. Harmuth, H., Rieder, K., Krobath, M., Tschegg, E., 1996: Investigation of the nonlinear fracture behaviour of ordinary ceramic refractory materials. *Materials Science and Engineering: A* 214(1-2): 53-61.
8. Johnson, J.A., 1973: Crack initiation in wood plates. *Wood Science* 6(2): 151–158.

9. Kang, C.W., Schwarzkopf, M., Muszynski, L., Jin, T., Park, H.J., Kang, H.Y., Matsumura, J., 2014: Mechanical behavior of separated earlywood and latewood of Douglas-fir using digital image correlation method. *Journal of the Faculty of Agriculture, Kyushu University* 59(1): 127–131.
10. Konukcu, A.C., Quin, F., Zhang, J., 2021: Effect of growth rings on fracture toughness of wood. *European Journal of Wood and Wood Products* 79(6): 1495–1506.
11. Kretschmann, D.E., 2008: The influence of juvenile wood content on shear parallel, compression, and tension perpendicular to grain strength and mode I fracture toughness of loblolly pine at various ring orientation. *Forest Products Journal* 58(7–8): 89–96.
12. Kretschmann, D.E., 2010: Mechanical properties of wood. In: *Wood handbook: wood as an engineered material* (ed. Ross R.J). Pp 1–46, chapter 5, Forest Products Society, Madison, WI.
13. Kretschmann, D.E., Cramer, S.M., 2007: The role of earlywood and latewood properties on dimensional stability of loblolly pine. *Proceedings of the Compromised Wood Workshop*. Pp 215-236, New Zealand.
14. Kretschmann, D.E., Green, D.W., Malinauskas, V., 1991: Effect of moisture content on stress intensity factors in southern pine. *Proceedings of the 1991 International timber engineering conference*. Pp 391-398, vol. 3, London.
15. Majano, M.A.M., Hughes, M., Fernández-Cabo, J.L., 2010: A fracture mechanics study of thermally modified beech for structural applications. *11th World Conference on Timber Engineering, WCTE*. Pp 989-990.
16. Mall, S., Murphy, J.F., Shottafer, J.E., 1983: Criterion for mixed mode fracture in wood. *Journal of Engineering Mechanics* 109(3): 680–690.
17. Nakao, T., Susanti, C.M.E., Yoshihara, H., 2012: Examination of the failure behavior of wood with a short crack in the radial-longitudinal system by single-edge-notched bending test. *Journal of Wood Science* 58(5): 453–458.
18. Ohuchi, T., Hermawan, A., Fujimoto, N., 2011: Basic studies on fracture toughness of sugi and acoustic emission. *Journal of the Faculty of Agriculture, Kyushu University* 56(1): 99–102.
19. Patton-Mallory, M., Cramer, S.M., 1987: Fracture mechanics: a tool for predicting wood component strength. *Forest Products Journal* 37(7/8): 39–47.
20. Porter, A.W., 1964: On the mechanics of fracture in wood. *Forest Products Journal* 14(8): 325–331.
21. Qiu, L.P., Zhu, E.C., Zhou, H.Z., Liu, L.Y., 2012: Fracture toughness of northeast China larch. *Key Engineering Materials* 517: 661–668.
22. Reiterer, A., Sinn, G., Stanzl-Tschegg, S.E., 2002: Fracture characteristics of different wood species under mode I loading perpendicular to the grain. *Materials Science and Engineering A* 332(1–2): 29–36.
23. Reiterer, A., Tschegg, S., 2002: The influence of moisture content on the mode I fracture behaviour of spruce wood. *Journal of Materials Science* 37(20): 4487–4491.

24. Schniewind, A.P., Centeno, J.C., 1973: Fracture toughness and duration of load factor I. six principal systems of crack propagation and the duration factor for cracks propagating parallel to grain. *Wood and Fiber Science* 5(2): 152–159.
25. Smith, I., Landis, E., Gong, M., 2003: *Fracture and fatigue in wood*. John Wiley & Sons, Inc. England, 234 pp.
26. Shmulsky, R., Jones, P.D., 2011: *Forest products and wood science: an introduction*. John Wiley & Sons. England, 477 pp.
27. Tan, D.M., Stanzl-Tschegg, S.E., Tschegg, E.K., 1995: Models of wood fracture in mode I and mode II. *Holz Als Roh-Und Werkstoff* 53(3): 159–164.
28. Thuvander, F., Berglund, L.A., 2000: In situ observations of fracture mechanisms for radial cracks in wood. *Journal of Materials Science* 35(24): 6277–6283.
29. Tschegg, E.K., Reiterer, A., Pleschberger, T., Stanzl-Tschegg, S.E., 2001: Mixed mode fracture energy of spruce wood. *Journal of Materials Science* 36(14): 3531–3537.
30. Tukiainen, P., Hughes, M., 2016: The effect of temperature and moisture content on the fracture behaviour of spruce and birch. *Holzforschung* 70(4): 369–376.
31. Watanabe, K., Shida, S., Ohta, M., 2011: Evaluation of end-check propagation based on mode I fracture toughness of sugi (*Cryptomeria japonica*). *Journal of Wood Science* 57(5): 371–376.
32. Wiedenhoef, A., 2010: Structure and function of wood. In: *Wood handbook: wood as an engineered material* (ed. Ross R.J). Pp 1–18, chapter 3, Forest Products Society, Madison, WI.
33. Yoshihara, H., 2010a: Examination of the mode I critical stress intensity factor of wood obtained by single-edge-notched bending test. *Holzforschung* 64(4): 501–509.
34. Yoshihara, H., 2010b: Influence of loading conditions on the measurement of mode I critical stress intensity factor for wood and medium-density fiberboard by the single-edge-notched tension test. *Holzforschung* 64(6): 735–745.
35. Yoshihara, H., Usuki, A., 2011: Mode I critical stress intensity factor of wood and medium-density fiberboard measured by compact tension test. *Holzforschung* 65(5): 729–735.

ARIF CAGLAR KONUKCU*
IZMIR KATIP CELEBI UNIVERSITY
FACULTY OF FORESTRY
DEPARTMENT OF FOREST INDUSTRIAL ENGINEERING
35620, IZMIR
TURKEY

*Corresponding author: arifcaglar.konukcu@ikcu.edu.tr